Chapter 5

Characteristics of Hurricane Ike During Its Passage over Houston, Texas

Gunnar W. Schade

Additional information is available at the end of the chapter

http://dx.doi.org/10.5772/51344

1. Introduction

Hurricane impacts, real and perceived, are most obvious when a hurricane makes landfall in populated areas. While hurricane track and strength forecasting has clearly improved in the last decade, increasing coastal development puts increasing population numbers in harm's way [1]. In addition, the modified coastal environment with its human infrastructure is affected by coastal flooding from the storm's surge, inland flooding from torrential rains, and damaging hurricane winds. Recent hurricane research has sought to characterize land-falling hurricanes better [2-7], particularly in order to understand the dynamics and development of hurricane winds during landfall and the associated potential for wind damage to structures and the natural environment. The necessary safety prerequisites to instrumentation observing land-falling hurricanes, and the amount of data they collect demand a high organization, quick response to meteorological developments, careful data analysis, and patience. Thus, as this research is only approximately a decade old few reports have appeared in the peer-reviewed literature so far.

Meteorological measurements inside urban areas are also relatively rare as guidelines for proper setup of representative weather stations usually lead to conflicts in such areas. However, meteorological measurements, as well as weather and impact forecasts in and for conurbations are becoming more important as urban populations increase. An increased (meteorological) focus has been put on the urban environment [8-12], and guidelines have been developed for urban measurements and site qualifications [13-15]. Micrometeorological observations in urban areas are especially challenging but many more observational data sets have been acquired in the last decade since Roth's seminal review in 2000 [9, 16]. One of these is being acquired in Houston, Texas, since summer 2007 as part of a project to study atmospheric turbulence, and anthropogenic and biogenic trace gas fluxes over a typical urban landscape

[17, 18]. Approximately a year after project measurements had begun, Hurricane Ike approached the Gulf Coast with a forecast track right through the City of Houston. While the author's installations on the communications' tower used for the study were designed to withstand high winds, the tower itself was not rated for a category three hurricane, and there was thus a good chance it would topple if Ike maintained its strength upon landfall. On September 12/13, 2008, at landfall near Galveston, Texas, Ike was finally rated "only" a category two storm on the Saffir-Simpson scale. The tower survived. However, due to the impacts of Ike's enormous size and wind field the storm caused widespread disaster and power loss to approximately 2.1 million customers in the Houston metro area [19], and is now considered the USA's second most costly hurricane in history at nearly 30 billion USD of estimated, accumulated damages [20].

A major impact of Ike to people and infrastructure in the Houston metro area stemmed from debris, both from natural vegetation and damaged human infrastructure [21]. Particularly the amount of damage to the energy (electricity) infrastructure was staggering, leaving sections of the metro area population without power for more than three weeks after the storm's passage [19]. What was highly visible in Houston long before the storm, and had been concluded by us as the major culprit [22], was the lack of proper tree trimming leading to tree-debris-caused power line failures. Within the first year after the storm, it had been concluded that this was indeed the leading cause for the amount of failures, and that in conclusion future activities would focus on appropriate tree trimming [23, 24].

As the instrumented communication's tower north of downtown Houston rode out the storm, albeit partially damaged, and power to the site was never lost due to a local diesel generator, it was possible to record meteorological and air quality data both during the storm and its aftermath. This chapter will focus on the storm's meteorological characteristics as measured over the urban area north of downtown Houston. They represent, so far, the only recorded hurricane passage over an urban environment [22]. Firstly, there will be a review of the installation's salient features and important past observations, followed by a brief description the hurricane's development. The following sections will focus on the development of Ike's winds over Houston in comparison to past findings, and their impacts in the neighborhood of the site. Lastly, connections between the hurricane's thermodynamics, its rainbands and winds, and air quality will be explored. A more detailed view of the latter shall be reported elsewhere.

2. The Yellow Cab tower site

The Greater Houston Transportation Co. owns and operates a 91 m tall communications tower at 1406 Hays Street, 77009 Houston, TX, approximately 3.5 km NNE of downtown Houston (29.789° N, 95.354° W, 14 m above sea level). In 2007 the tower was equipped with meteorological and micrometeorological instrumentation to measure standard meteorological parameters plus atmospheric turbulence and surface energy exchanges. In June 2008, the existing 4-level gradient measurements were expanded by a level at 49 m above ground level (agl), and an extra sonic anemometer at 40 m agl. Details of the instrumentation can be found in [17], downloadable from the project's website. On the top level, a MetOne model 034B wind speed

http://dx.doi.org/10.5772/51344

(ws) and direction (wd) sensor was used, and on the lower levels MetOne 014A ws only models with standard metal cups were used. Both sensors have a starting threshold of <0.5 m s^{-1} and distance constants of <= 4.5 m, equivalent to a 95% of maximum response time of approximately 3 seconds in a typical 9 m s^{-1} wind. Data were recorded in 10-s intervals and stored as 1-min averages and standard deviations except atmospheric pressure, which is only recorded every 15 minutes, but was smoothed for the analysis purposes of this study. Micrometeorological data from the installed sonic anemometer at 60 m agl was recorded at 10 Hz up to approximately midnight on 12 September 2008 when increasing rainfall began to completely cut the signal. The sonic anemometer then did not recover until two days after the storm. Rainfall was recorded with a tipping bucket (model TE525) on the E side of the tower, ten meters agl, and atmospheric pressure from within the data logger enclosure at two meters agl. Lastly, carbon monoxide was measured by a model 48CTL gas filter correlation instrument, corrected for background drift every two hours and calibrated once a week (precision ±20 ppb). The instrument samples air from inlets at 40 and 60 m agl on the tower.

Figure 1 shows a picture of the instrumented tower in summer 2008 (a), and a bird's eye view of the surrounding area with labels (b). A more detailed description of the underlying urban surface is given in [25] and our TARC report [17]. Of particular interest with respect to wind measurements is the location of the sensors relative to the lattice tower structure itself. Figure 2 shows the setup on the top level (60 m agl) and an example of the lower level installations.

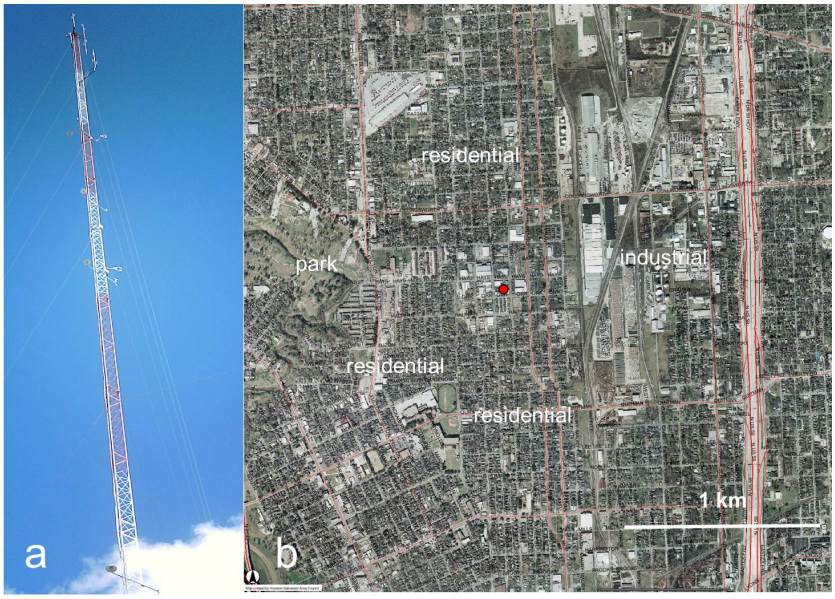

Figure 1. a) Picture of the top four meteorological installations on the flux tower during summer 2008. Note temporary installation of an additional sonic anemometer at the 40 m agl. (b) Annotated bird's eye view of the tower location (red dot) north of downtown Houston. Red lines indicate major thoroughfares.

As the wind climatology for Houston indicated rare occasions of northerly winds, the sonic and the lower level cup anemometers were installed on the south side of the tower. The top level ws/wd sensor was installed as a "backup" sensor on the NW side of the tower. As shown in Figures 1&2, the triangular tower lattice structure has a side length of 60 cm (2 ft), thus is bound to affect wind flows towards the cup anemometers for average wind directions between approximately 320 and 10 degrees as the sensors are within three times the largest horizontal tower dimension. A similar argument holds for the sonic anemometer at similar wind directions, and for the ws/wd sensor for SE wind directions. Though the effects may be smaller in both the latter cases due to larger distances from the tower, there is an additional electronics box installed on the tower at that level, which can cause an extra wake.

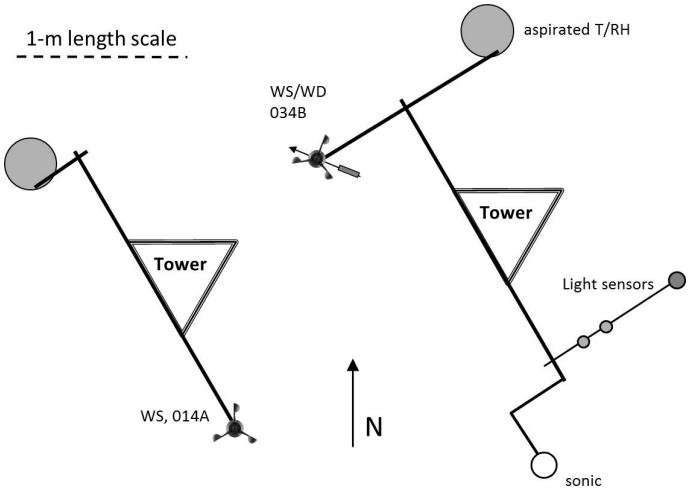

Figure 2. Meteorological instrumentation installed at the Yellow Cab tower in Houston at 60 m agl (right), and the lower levels (49, 40, 20, 13 m agl; left). The tower has a side length of 2 ft with vertical bars of 1 ½ inches diameter. Installed horizontal beams (solid black lines) consist mostly of aluminum pipes (Campbell Scientific Inc., Logan, Utah, USA). Note that the aspirated radiation shields (MetOne model 075B) are installed with an off-center beam.

Measurements from the tower since late summer 2007 were used to determine the structure of atmospheric turbulence at this urban site, and the underlying surfaces' roughness lengths (z_0) and displacement heights (d). Figure 3 shows the observed behavior of normalized longitudinal and vertical winds – as relevant for this study – with the atmospheric stability parameter ζ=(z-d)/L for daytime unstable conditions, where is z is measurement height and L is the Obhukov length. We observed surprisingly low directional heterogeneity in the data, thus these results were pooled. A comparison to the review of Roth [16] listed in Fig. 3 showed few differences as compared to past findings over urban areas.

A combination of methods to determine z_0 and d [26] was used to arrive at values of $z_0 = 1 \pm 0.1$ m, and $d = 8^{+3}_{-2}$ m [17]. The distribution of values together with an analysis of building and tree heights in the area revealed that d is dominated by the tree canopy in this area [17]; details will

http://dx.doi.org/10.5772/51344

be published elsewhere. Some heterogeneity was observed for heat and trace gas fluxes, but details shall also be given elsewhere. Here, the surface heterogeneity in the immediate surroundings of the tower is relevant: Within a radius of 150 m, the surface is largely impervious and dominated by warehouse-style buildings with different roof angles and heights. The tallest building is a large, approximately 50×70 m^2 structure to the NW that can be easily spotted in Figure 1b. There are very few tall trees within a 100 m radius from the tower.

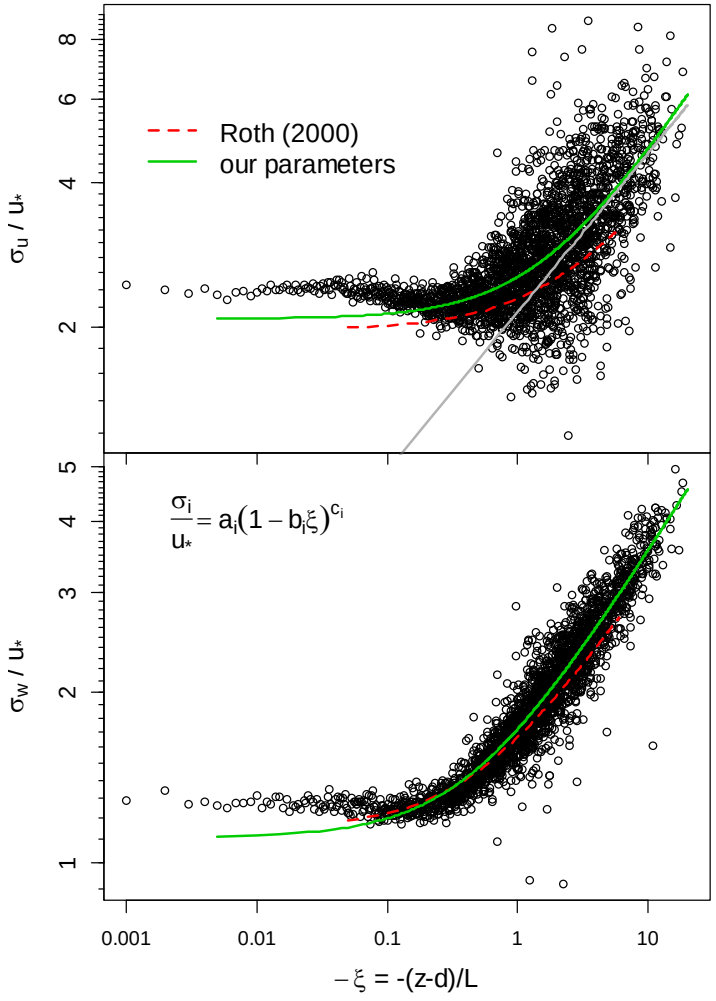

Figure 3. Normalized longitudinal and vertical wind standard deviations as function of atmospheric stability for unstable conditions, compared between our site and other urban data as summarized by Roth [16]. The grey line shows the expected c_i=⅓ slope. For all i=u,v,w, we observed neutral stability values close to the literature data, namely 2.4, 1.8, and 1.3.

Despite some obvious surface heterogeneity, the lack of significant directional differences in the measured turbulence can be explained by the z=60 m agl measurement height, which is approximately six times the displacement height and therefore well above the recommended height for such measurements [16], inside the inertial sublayer. This height was initially chosen to integrate our flux measurements over a larger, more representative urban surface area. Flux footprint estimates [25] indicate that under typical wind speeds (4-6 m s^{-1}) and turbulence conditions (friction velocity, u_*=0.4-0.6 m s^{-1}) at this site, 90% of measured fluxes are expected to come from less than 1.5 km distances, with maximum impacts from locations <=500 m from the tower [25], and total footprint sizes of 2-4 km^2. However, for wind speeds between 20-30 m s^{-1} and associated turbulence discussed below, maximum impact areas move significantly closer to the tower (<=350 m) and footprint size contracts, so that a larger effect of the surface and its heterogeneity close to the tower on the measurements is to be expected. This is also evident through a decrease of the displacement height with observed wind speeds (or friction velocities) [17], likely because of the lack of tall trees closer to the tower.

3. Hurricane Ike

Ike was a somewhat uncharacteristic hurricane due to its very large eye and wind field, filling nearly the entire Gulf of Mexico on 12 September 2008. Though its wind speeds classified Ike as a category two hurricane at landfall (maximum winds between 96 and 110 mph = 43-49 m s^{-1}), a more holistic view called the *hurricane severity index* [27] ranks it similar to such disastrous landfalling hurricanes as Andrew in 1992 and Ivan in 2004. Most of Hurricane Ike's history and measures, including its track, precipitation, and measured or estimated winds are described online [28], and shall not be repeated here. A track map through Houston and a brief analysis of our meteorological data were also given earlier [22]. For comparison purposes to this study, Figure 4 shows two important meteorological variables: Fig. 4a shows a precipitation radar image (KHGX Houston, located at the green-blue dot south of the eye) from the period of maximum wind speeds, approximately one hour before the minimum locally measured pressure at the tower site; Fig. 4b shows gridded, calculated maximum sustained wind speeds for Harris County, assembled from the original GIS data [28], which have generally been shown on a much larger scale [27, 29]. Note that Ike preserved its very large eye for a comparatively long time after landfall, and that the City of Houston, roughly outlined by the *Beltway*, was well within Ike's eyewall. As a result of this, several additional rain bands passing over, and the flat Texas coastal terrain, widespread flooding occurred in central and north Houston. Particularly, the *White Oak Bayou* watershed area, at the SE corner of which the tower site is located, was listed as "Major Flooding / House flooding area from rainfall". The same area was calculated to have experienced category one (74-95 mph = 33-43 m s^{-1}) hurricane wind speeds, with a maximum of 38 m s^{-1} estimated for the tower site and much of central Houston (Fig. 4b). However, it needs to be pointed out here that these are NOAA AOML Hurricane Research Division (HRD) *surface wind* data that are – in this case – valid only for "open terrain exposure over land". They are a standardized product reflecting speeds at 10 m

http://dx.doi.org/10.5772/51344

agl for a flat surface (d=0) without significant roughness elements (z_0<=0.1 m). Actually measured speeds are discussed below.

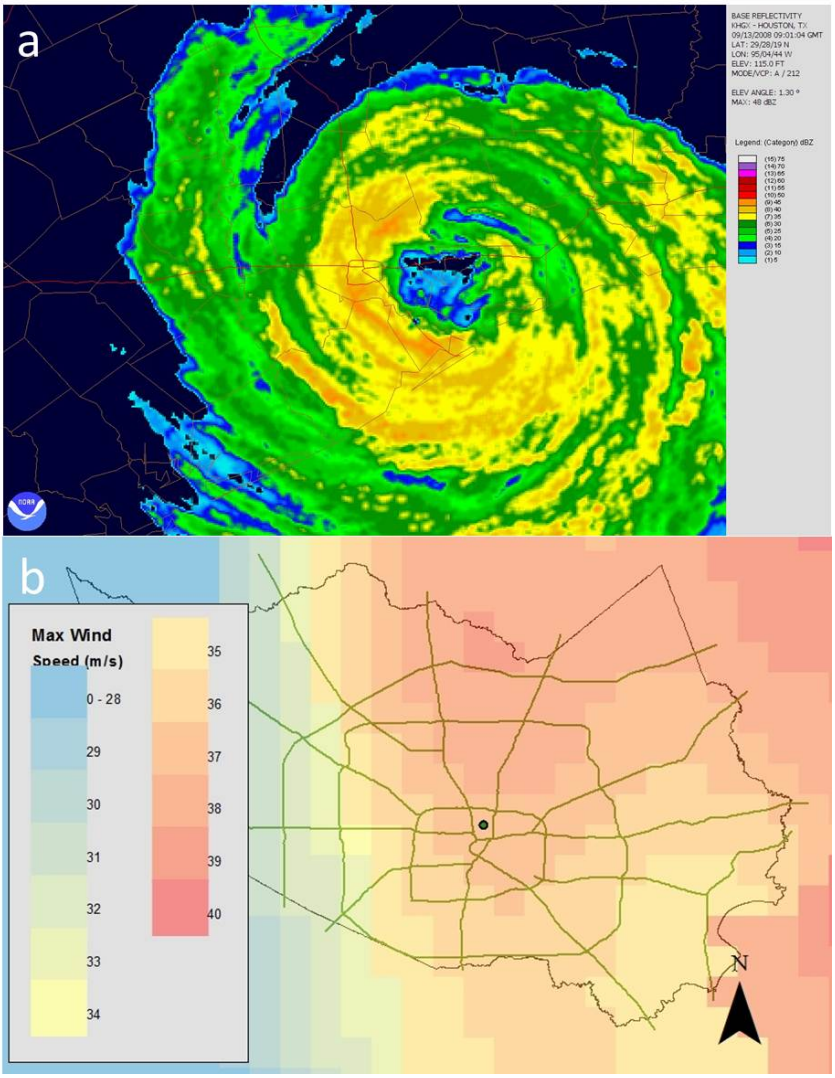

Figure 4. a) Precipitation radar image from 13 September, 09:00 GMT (03:00 CST) overlaid on a Texas county map (grey lines) and including interstate highways (red lines), the circular one in the center depicting Houston's *Beltway*, which extends for approximately 19 km in its E-W direction. (b) Maximum sustained wind speeds (NOAA Atlantic Oceanographic & Meteorological Laboratory Hurricane Research Division H*Wind product) during Ike in Harris County, Texas, overlaid on the county border (black line) and major thoroughfares (green lines). The central dot marks the tower location.

4. Wind measurements

4.1. Wind speeds and turbulence intensities

In Figure 5 are depicted measured wind speeds at 60 and 20 m agl from the Yellow Cab tower for 12th (DOY 256) and 13th (DOY 257) September 2008. Wind direction is included in the form of arrows along the bottom, and approximate timing of rain band passages along the top of the graph. For northerly winds, which occurred in the afternoon of DOY 256 and for approximately four hours around midnight at the height of the storm, the measured 20-m agl wind speeds are clearly impacted by the tower structure as explained above. As the eye passed and wind direction shifted to the NW, the sensor moved out of the tower's wake, and recorded its highest 1-min values of 22-25 m s^{-1} around 4 am Central Standard Time (CST = CDT - 1 h). This timing will be addressed again below.

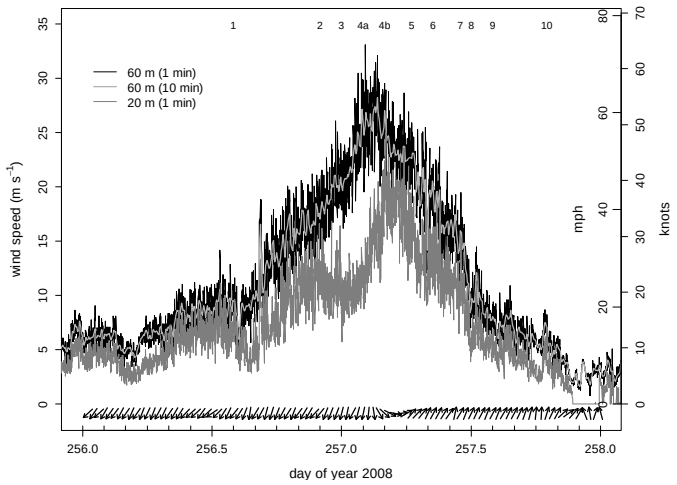

Figure 5. Measured wind speeds during Hurricane Ike's passage over Houston on September 12-13, 2008. Arrows along the bottom depict wind direction, numbers on the top locate the timing of rain band passages with labels 4a and 4b identifying the eyewall.

Considering a displacement height of close to ten meters for our site, the 20-m agl measurements come closest to the standardized H*Wind product shown in Fig. 4b. The large difference between the two (25 vs. 38 m s^{-1}) is associated with the higher urban roughness length. Higher roughness lengths increase surface friction and therefore reduce wind speed.

Fig. 5 includes 10-min average wind speeds for the top level sensor and therefore allows a direct comparison between sustained winds and 1-min gustiness (10-s mean winds were not recorded). Only the latter revealed hurricane-force winds (>33 m s^{-1}) at the top level, 60 m agl, while sustained (10-min) tropical storm force winds (>17 m s^{-1}) were recorded for nearly 12 hours. However, extrapolating sustained top level to the 20-m agl wind speeds using the log-wind-law

http://dx.doi.org/10.5772/51344

$$\hat{U} = u* / k \times \ln\left((z\text{-}d) / z_0 \right) \quad (1)$$

where $\hat{U}$ is 10-min average wind speed, u_* is friction velocity, and k=0.4 is von Karmann's constant, reduces the time of 17+ m s^{-1} wind speeds to a mere 15 min. This analyses shows that the rough urban surface was very efficient in slowing down Ike's winds. Other surface maximum wind speed observations in the Houston urban area, compiled by Berg [20], ranged from 16 (west Houston) to 65 (Houston Hobby airport, south Houston) knots (see Fig. 5 for speed conversions), confirming that hurricane force winds were rare in the urban canopy even in the eyewall.

Higher surface roughness in the urban area though increases atmospheric turbulence. The latter was analyzed in two ways, investigating drag or wind force, and turbulence intensities, I_U. The former was calculated following [30], also cited in [31], from the 20-m agl sustained wind speed data in combination with air density. The latter was calculated from 15-min non-overlapping segments for both the sonic and cup anemometers, except during the last six hours before midnight when lower data density due to rain required half-hourly or hourly averages. In Figure 6 we plotted the resulting wind force per area and its standard deviation. Mean values characterize *static*, while fluctuations characterize *dynamic* wind load on surface roughness elements. Under "normal" conditions (DOY 256 morning), loads rarely exceed 1 kg m^{-1} s^{-2}, but during the hurricane, loads increased by a factor of 5-10 in the eyewall.

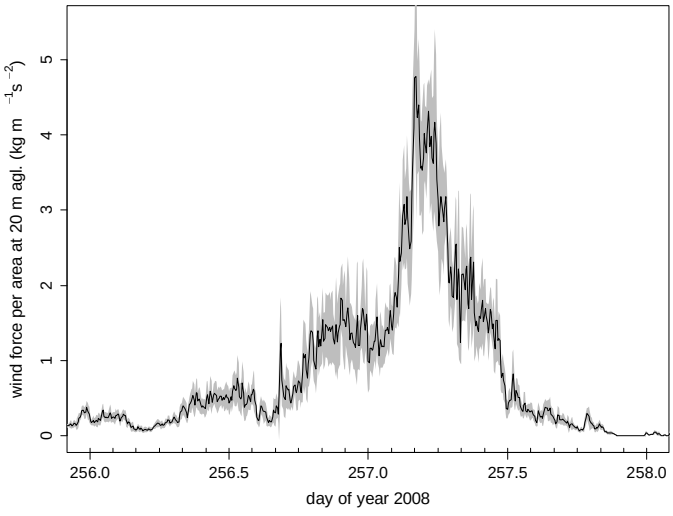

Figure 6. Wind force, proportional to $\hat{U}^2$, time series during Hurricane Ike's passage over Houston. The grey swath is an estimate of its standard deviation.

In Figure 7 are plotted turbulence intensities time series as calculated from the sonic anemometer data and the top level wind sensor, alongside the storm's pressure, wind direction, and rain band timing characteristics. Due to the higher data density of 10 Hz vs. 0.017 Hz, values

are much larger for the sonic vs. the cup anemometer. Prior to the storm, I_U is influenced by atmospheric stability, leading to higher values during daytime unstable conditions. Values further increased when wind direction was northerly due to a reduction in wind speed but not its standard deviation in the tower's wake. Sonic-derived longitudinal (I_u) and lateral (I_v) turbulence intensities can be compared to the high frequency data obtained from anemometers installed near the coast line during the landfall of other hurricanes [3-6, 32].

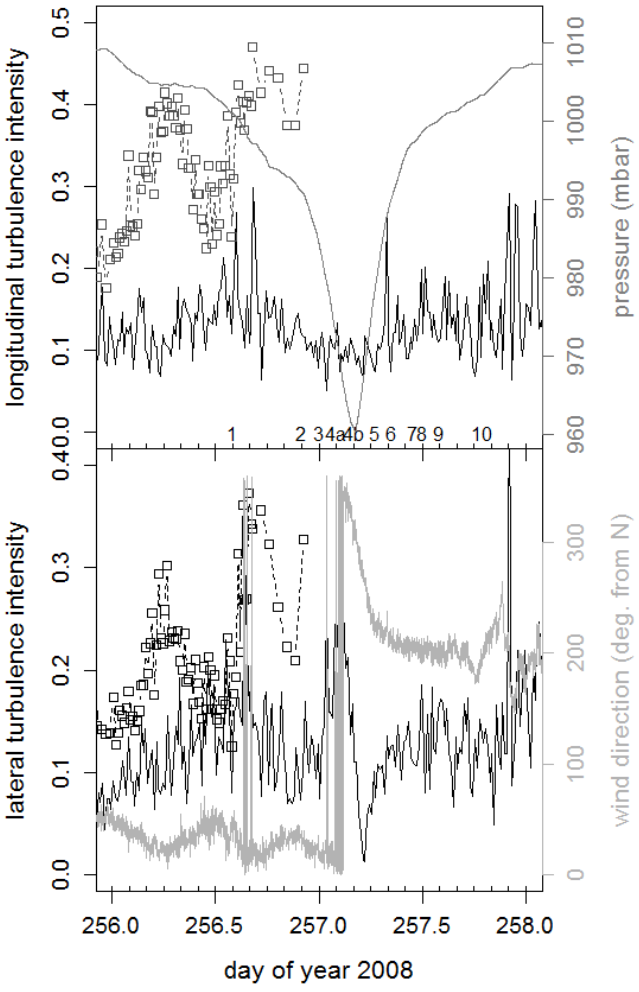

Figure 7. Turbulence intensities as measured by the sonic and top level cup anemometers as compared to storm passage characteristics of pressure (top panel) and wind direction (bottom panel). Lateral turbulence intensity of the 034B sensor depicted in the bottom panel is assessed from the 1-min wind direction fluctuation (right axis) and plotted as $10\times\sigma_{wd}/360$ (left axis). Note the surprise lull under northwesterly wind directions towards the end of the eyewall passage.

http://dx.doi.org/10.5772/51344

As expected, values are, in general, larger than those obtained over the relatively smooth surfaces encountered in those previous studies. However, the expected dependence of I_U on surface roughness length is clear also in previous data [6]. In addition, I_U also depends on measurement height and wind speed. Turbulence intensity data obtained from a tall tower over urban Beijing [33] are roughly consistent with the above results, I_u = 0.3-0.4, and I_v=0.25-0.35 at similar measurement heights. However, while a mean I_v/I_u ratio of 0.87 was obtained, other studies such as [33]and [6] obtained 0.75, close to the expected value from MO theory, suggesting that the tower's wake influences reduced I_u more strongly than I_v. Nevertheless, use of the predictive formulas listed in [33] to compare the results to resulted in a reasonable fit using the formula

$$I_u = 0.765 \times \left(10/z\right)^{0.447} \tag{2}$$

which leads to a value of 0.34 compared to a mean measured value of 0.29±0.09 (1 sd), not including wake-affected values for the two days entering the calculation (DOYs 255&256).

Wind speed influences on I_U can be observed from the top level cup anemometer data. As the storm approached, I_U dropped slightly and became less variable, more or less consistent with the pressure development. A similar result was presented in [33] for winds measured over Beijing, while not as clear for the coastal hurricane land fall measurements [4, 6].

A closer inspection of observed wind speeds and associated turbulence intensities in Figures 5 and 7 shows that rain band passage affected both measures. Wind speeds increased just prior to or shortly after rain band passage. Spikes are visible both prior to and after the first outer rain band passed over Houston, as well as prior to nearly all outer rain band passages. A similar argument can be made for the eye wall passage itself: Label 4a characterizes passage of the NW side of the eye wall, while label 4b characterizes passage of the SW side of the eye wall. Both were associated with heavy rainfall, but the period in between experienced slightly lower rainfall rates. In all these cases, short-term increased wind speeds were likely associated with mesoscale circulations within the storm associated with descending air between rain bands accelerating towards an inner rain band. Convection inside the rain band causes heavy rainfall and was generally associated with lulls in wind speed. In contrast, as can be seen from Figure 7 it was often associated with short-term increases of turbulence intensity as a likely effect of stronger convective activity.

4.2. Mesoscale storm characteristics

With increasing wind speed in storms, large scale wave structures are expected to form, often called *rolls*. These have been investigated for hurricanes before through Doppler radar, integral length scales (L_x, x=u,v,w), and wind speed spectral analyses [2, 5-7, 34]. Several of these authors found that both sub-kilometer and meso-gamma scale (several kilometers) features can be observed in hurricanes. Compared to observations at lower wind speeds, these features lead to higher values at lower frequencies in the (normalized) wind power spectrum, particularly between 0.01 and 0.001 reduced frequency values. Some of these analyses have been

repeated here; however, the loss of sonic anemometer data during rain prevents a detailed spectral analysis, and the data acquisition frequency of the cup anemometers limits integral length scale and spectral analysis.

R software [35] was used to calculate normalized, partially smoothed spectra from 2-hour detrended segments of both sonic and cup anemometer data. Integral length scales were calculated from the sonic data by (i) selecting non-overlapping 10-min segments and calculating the auto-correlation function (acf), (ii) fitting an exponential decay curve to the acf, and (iii) integrating the exponential function out to twice the first zero-crossing observed in the acf. The procedure was similar to that described in [6] and [4].

Here, pre-storm wind speed spectra from both the top level sonic and cup anemometers were compared to height-of-storm cup anemometer data. A short-coming of the previous works is the lack of comparison between observed hurricane wind spectra and "normal" wind speed spectra at the same locations. Figure 8 shows the calculated power spectra for the 2-h, neutral stability longitudinal wind segments.

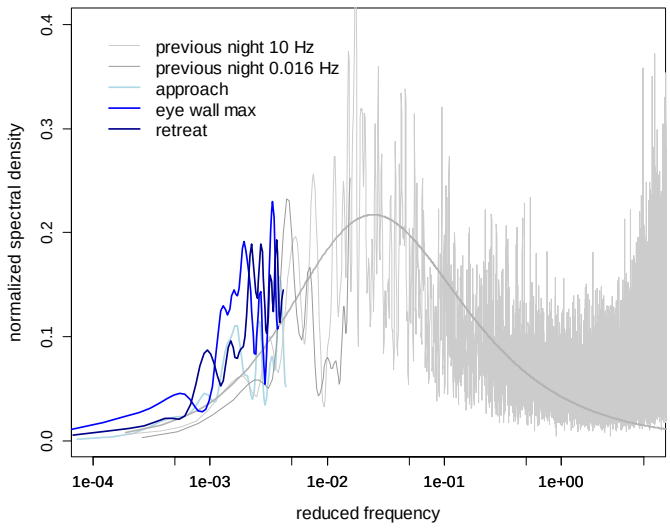

Figure 8. A comparison of longitudinal wind speed spectra between the night before the hurricane (DOY 256, hours 01:00-03:00 CST) and three periods of the highest encountered wind speeds before, during, and after the eyewall maximum. Smoothing was limited to highlight differences. The thick, dark grey line represents a standard spectrum. Note that the grey spectra from the previous night were obtained at an average wind speed of 6 m s^{-1}, the offset being due to a slightly higher value recorded by the cup anemometer. Wind speeds for the blue spectra were all above 22 m s^{-1} (Fig. 3). To match power density levels (y-axis) the blue spectra were additionally normalized to the wind speeds' standard deviation ratios.

The grey spectra match surprisingly well between the top level sensors at lower frequencies. At the same time, they are well characterized by the standard, smoothed "perturbed terrain" model spectrum [4], which shows a maximum at 2-3×10^{-2} and falls off below

http://dx.doi.org/10.5772/51344

1×10^{-2}. In comparison, the visible meso-gamma scale features at reduced frequencies between $1\text{-}5\times10^{-3}$ were strongly enhanced in the high wind speed spectra. This is consistent with the previous findings [4, 7]. For the wind speeds encountered here, these are features with wavelengths between approximately one and five kilometers, and might be associated with boundary layer rolls.

Previous analyses of hurricane winds integral length scales, corresponding to the frequencies of maximum power in the power spectrum, ranged from less than hundred to several hundred meters for L_u, but were all observed over relatively flat terrain or with ocean fetches [2, 4, 6, 7]. Comparative length scale data to the one observed in Houston come from the Beijing tall tower measurements [33]. That study reported highly variable values with means of approximately 100 and 200 m for z=47 and 120 m agl. Similar to the data above, that data base contained only wind speeds up to 15 m s^{-1} at z=120 m, but the authors did not analyze for wind speed correlation. As integral length scales were found to increase with wind speed [7] it is possible that larger average length scales would have resulted had wind speeds been higher. Here, length scale data were calculated between noontime on DOY 256 and midnight under the limitations described above. The results are summarized in Table 1.

Length scale	this study (mean ± sd)		Li et al. (means)	Yu et al. (mean ± sd)	Masters et al. (mean ± sd) 1
	all data	wake-free data			
L_u	217±168	282±185	104, 195	122 ± 29	130 ± 45
L_v	177±137	214±153	44, 93		90 ± 43

[1]these values are averages over several landfalling hurricanes; the actual spread of the values for each hurricane was at times much larger than indicated by the sd of the means listed here

Table 1. Integral length scales in meters for winds <= 15 m s^{-1} (this study and [33], $z_0\approx1$ m), and >=15 m s^{-1} ([6] and [7], $z_0<0.1$ m)

The observed values are broadly comparable. Similar to all observations is the relatively large variability of the data, with several values exceeding 400-500 m length scales, and a generally log-normal distribution. A slight dependence on wind speeds and a good correlation between L_u and L_v was observed in this study's data and the data in [6]. The wind speed correlation suggests that values over 400 m should occur regularly for wind speeds exceeding 15 m s^{-1}, which is consistent with observations in [6]. The values over Beijing appear lower, but were likely influenced by a large amount of data at lower wind speeds, but this was not elaborated on [33].

4.3. Impacts

Sustained wind speeds and turbulence intensity account for the wind loads plotted in Figure 6. Typically, static loads exceed dynamic loads. However, dynamic wind loads can contribute significantly due to the increased turbulence created by wake effects of buildings in urban areas. Individual periods during which I_U was increased [17] locally were previously highlighted and discussed above. However, a single site measurement cannot assess all local effects. Where and when damages most likely occur has instead been assessed through standardized measurements and models in the past. For instance, the results from extensive works on wind-throw in forests in [30, 36, 37], [38], [39], and [31] may be applicable to urban areas because, as in Houston, urban tree distribution is often patchy. In addition, buildings represent additional roughness elements causing similar or stronger wakes than other trees and stands in parks. While wind loads in Houston (Fig. 6) were seemingly not high enough to uproot trees, another measure to gauge surface impacts is momentum transfer or, more generically, (surface) friction velocity, u_*.

Friction velocity was measured directly with the sonic anemometer, but also calculated by linearizing the log-law (equation 1) for 10-min section mean winds using the four measurement levels from 20-60 m agl. If the preset roughness length and displacement height values are correct, the linearization retrieves friction velocity from the slope of the curve and a near zero intercept under neutral and near neutral stabilities, including some allowance for error (e.g. ±1 for the intercept). The results are plotted in Figure 9. We found a generally excellent match between the sonic anemometer and the wind gradient values.

Biases were observed for three reasons: First, when strong instability is present, such as visible midday on DOY 255. Second, during periods when wind speeds at the lower levels are affected by the tower's wake, generally between approximately 320 and 10 degrees; u_* is first under-, then overestimated and a negative, then positive y-intercept in the linearization is observed. This can be explained by a temporary acceleration the wind undergoes approaching the sensor from close to the tower structure for approximately 0-10 deg. N. This increases the linearization slope and creates a negative intercept. As wind direction turns further N towards NNW, winds are slowed through the tower structure, which creates a lower slope and a positive intercept. In either case, large residuals and poor determination coefficients of the linearization resulted. In neither case were winds at the top level affected. Third, the strongest bias though was observed for NW wind directions during the latter part of the eyewall passage, marked by the vertical dashed line. Calculated u_* plummeted and large positive intercepts were found from the linearization. At the same time, lateral turbulence intensity, I_v, dropped strongly, see Fig. 7, while strong updrafts turned the saucer-shape radiation shields from their horizontal into a vertical position (pictures are available online). For these wind directions, the flow advects over the large industrial building in 100 m distance, which occupies a significant fraction of the footprint at these wind speeds and likely produces a significant wake and associated turbulence. If only the top level sensor were affected at this wind direction, the linearization determination coefficient would again have been low and residuals high. This was, however, not the case. Thus, surface characteristics for this wind direction are most likely not well described by the preset z_0 and d values for the encountered wind speeds.

http://dx.doi.org/10.5772/51344

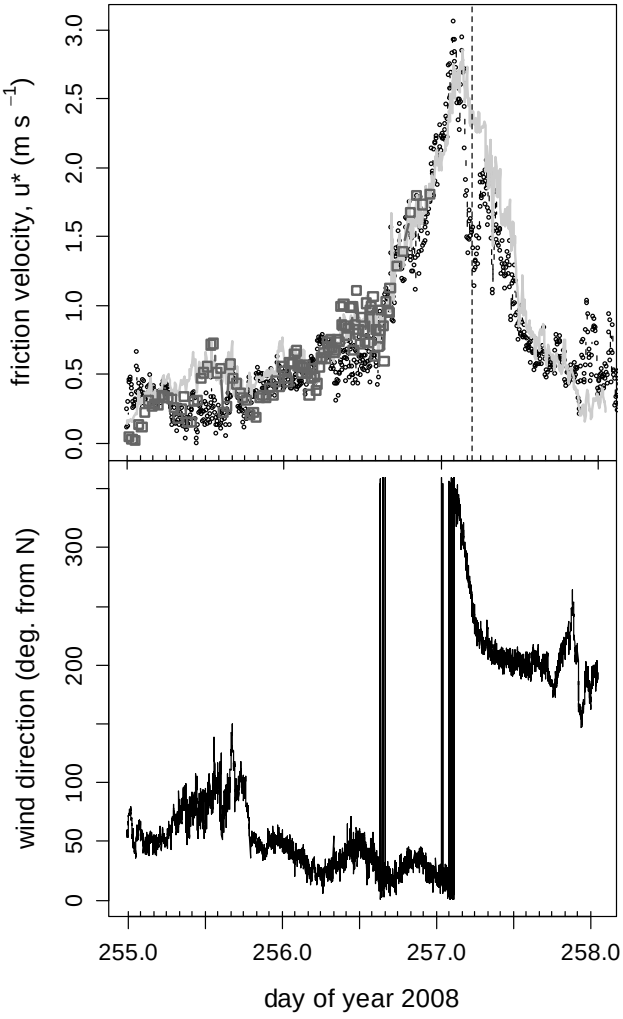

Figure 9. Friction velocity (upper panel) and wind direction (lower panel) time series during Hurricane Ike's passage over Houston. Small black circles depict all gradient-calculated values, open dark grey squares represent sonic-measured values, and the light grey line is a straightforward calculation of u_* using the log-law and only top level cup anemometer winds alongside preset z_0 and d. The vertical dashed line marks the period when winds advected from over the large building on the NW side of the tower.

In summary, Figure 9 shows extremely high, not previously measured friction velocities over an urban area. The corresponding large, turbulent downward momentum fluxes are the main destructive force in this environment. The results were observable after the storm. Figures 10 and 11 show the typical impacts in this neighborhood that led to the large scale power failures suffered all over the metro area.

Figure 10. Tree damage and debris along Hardy Road, ca. 2 km from the tower site.

Figure 11. View from the tower at 12 m agl towards NNW. The circles mark tree damage, the arrow on the lower left marks the local generator's exhaust pipe.

Two of the three tall trees immediately north of the tower, shown in Figure 11 growing alongside Hays Street between some of the larger buildings, and immediately downwind of the largest building in the area seen on the left, were also severely damaged, the one on the left losing nearly its complete crown.

http://dx.doi.org/10.5772/51344

It is also interesting that damage was largely confined to trees, or secondary damage from falling trees; significantly less (tile) roof damage was reported. This has previously been interpreted as being due to a mature tree canopy extending beyond roofs in many parts of Houston [40], with the trees taking the brunt of the storm's winds. However, in heterogeneous building areas such as the immediate surroundings of the tower site, small scale damage proportional to the encountered tropical storm force winds was caused. As shown in Figure 12, the local Yellow Cab headquarters suffered from a torn-off metal roof and a collapsed metal awning. In addition, not shown here, the company's antennas on top of the tower were bent and the tower's guy wires were loose, leading to significant sway of the tower. Similar damage kept cell-phone tower crews busy for months after the storm.

Another significant impact of hurricanes at landfall is the often torrential inland rainfall, leading to flash-floods and potential inundation of low lying areas. In this case, Houston was much more prepared, having learned lessons from many past floods, particularly tropical storm Allison in 2001. The next section will discuss Hurricane Ike's thermodynamic properties and the associated rainfall as compared to independent measurements.

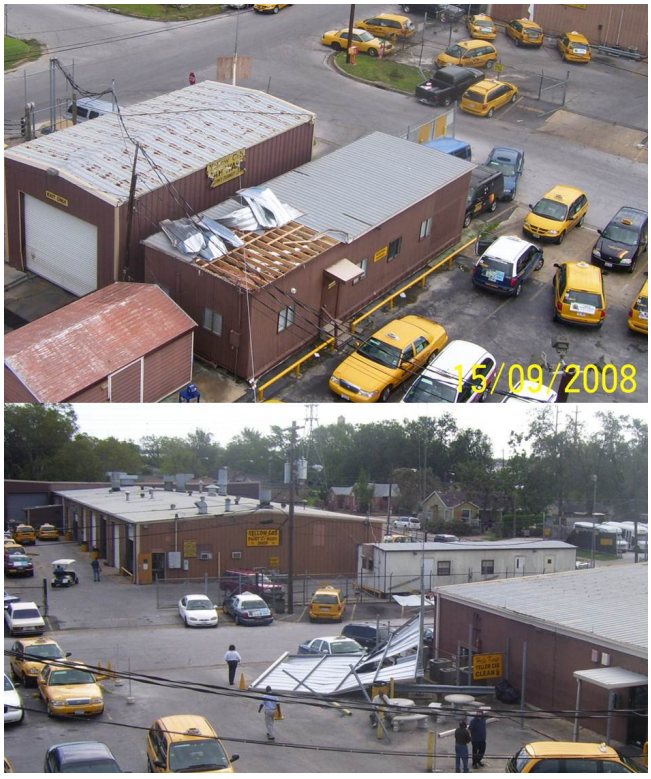

Figure 12. Structural damage caused by Ike as viewed from the tower at approx. 18 m agl towards NE (top) and ESE (bottom)

5. Equivalent potential temperature and rainfall

Hurricanes have been called equivalents of heat engines [41]. A warm ocean in disequilibrium with the overlying (dry) air supplies large amounts of water vapor by evaporation at the ocean surface. When condensing in the atmosphere this energy is released as latent heat of vaporization during air flow towards a pressure minimum, and it is efficiently converted into kinetic energy, i.e. increasing wind speeds. Conservation of angular momentum forces these winds to spiral faster as they approach the low pressure center of the storm. Increased wind speeds also cause increased evaporation of surface ocean water, maximizing humidity towards the center of the storm, where often the most heavy precipitation occurs. The increase of entropy towards the storm's eye can be depicted by calculating equivalent potential temperature (Θ_e), the temperature an air parcel would assume when brought adiabatically to surface reference pressure (potential T) and using latent heat of vaporization from condensing all its available water vapor to heat it. The distribution of Θ_e for a mature, symmetric hurricane over a uniformly warm ocean surface is presumably also close to symmetric, increasing towards the eyewall, and observational studies tend to confirm this structure, e.g. [42]. When hurricanes make landfall, their source of (latent heat) energy at the surface is cut off and drier air is eventually imported into the storm, leading to its inevitable dissipation over land. At a single measurement location, the 2-D thermodynamic structure of the hurricane can be observed via Θ_e when it moves past the sensor. Here, Ike's track allowed for this observation from the time of its approach to the coastline to its passage into northeast Texas. In Figure 13, Θ_e is plotted alongside measured precipitation and wetness. The wetness sensor typically allows for the detection of light rain when there was not enough rainfall to be detected by the tipping rain bucket instrument.

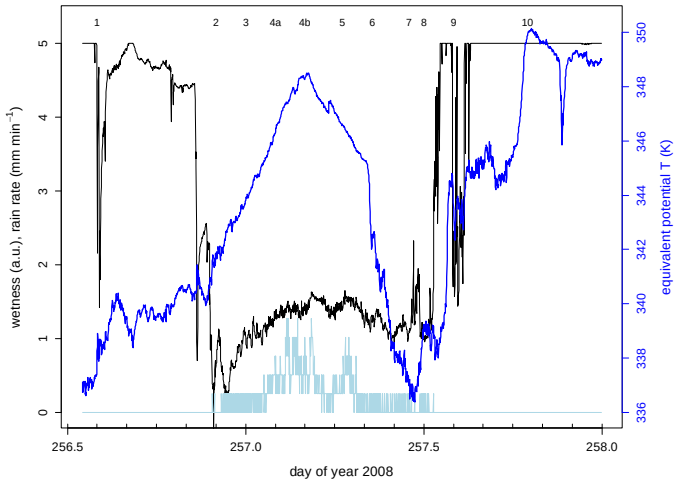

Figure 13. Time series of Θ_e (thick blue line), precipitation (light blue line), and wetness (thin black line) during Hurricane Ike's passage over Houston (wetness is plotted as the logarithm of the raw sensor signal, a resistance measurement). Similar to previous plots, radar-based evaluation of rain band passage timing is plotted along the top with bands 4a and 4b representing the eyewall.

http://dx.doi.org/10.5772/51344

It is clear from Fig. 13 that Θ_e near monotonously increased during the storm's approach and into its eyewall. Rapid increases were observed in the outer rain bands, including bands 8 to 10 in the afternoon after landfall, when the storm's center had migrated into northeast Texas and local precipitation had all but ceased. Increases in humidity as indicated by the wetness sensor were often clearly related to increases in Θ_e. Significant precipitation began to fall at the site shortly before 22:00 CST, and increased steadily into the eyewall. The highest rain rates were observed in the NW side of the eyewall, coincident with the highest wind speeds under still rising Θ_e levels (03:00 CST), and on the SW side of the eyewall just after the lowest pressure had been observed (04:00 CST). Then Θ_e rapidly dropped, and despite a short-term increase in an outer rain band with heavy precipitation (#5) fell to pre-storm levels before midday on DOY 257. The following afternoon rise, though associated with outer rain bands of the storm, was not associated with strong winds or significant precipitation any more.

This development, including its correlation with the winds as shown in Fig. 5, can be interpreted through the air circulation into the storm during and after landfall. For a straightforward elucidation, we carried out both a back trajectory analysis using HYSPLIT [43, 44] with 40 km resolution EDAS data, and an analysis of locally measured carbon monoxide concentrations as a tracer of continental air masses. In the first hours after landfall up to the approach of the eye closest to central Houston, the observed air masses were tropical marine in origin. As the storm approached the site it "imported" its Θ_e onto land. Beginning at approximately 04:00 CST, when the eye lay east of the tower site, the storm began to entrain drier continental air from north and northwest Texas into its western eyewall, which can explain the rapid decline in Θ_e. Figure 14 shows two back trajectory ensembles, one for just before the Θ_e decline, and one for six hours after decline had begun. This entrainment explains why Ike maintained much stronger wind speeds particularly on its eastern side throughout the morning [28] as this side continued to be fueled by Gulf of Mexico air masses. With the storm moving further north by midday and into the afternoon, wind direction had changed back to southerly flows with all air mass origins returning to the Gulf of Mexico (data not shown). This analysis is corroborated by the carbon monoxide data shown in Figure 15.

Typical continental boundary layer CO levels for September of 100-130 ppb were measured on DOY 256, with higher values during the morning and afternoon rush hour periods. As the storm approached and a tropical marine air mass was established, CO dropped to northern hemisphere marine background levels near 75 ppb, among the lowest levels measured in Houston. However, shortly after Θ_e levels began to drop and wind speeds plummeted, CO levels rose again to levels consistent with entraining continental air. Thus, the west side of the storm was rapidly deprived of its latent heat energy source. Nevertheless, short-term, small fluctuations in CO abundance, anti-correlated with Θ_e, could still be observed during the early afternoon of DOY 257. Later on, the reason for continued CO increases even after air mass origins had fully returned to tropical marine in the afternoon of DOY 257 can be found in a low nighttime boundary layer and large local CO emissions from electricity generators in the Houston metro area [45], including Yellow Cab's own onsite diesel generator (see Fig. 12).

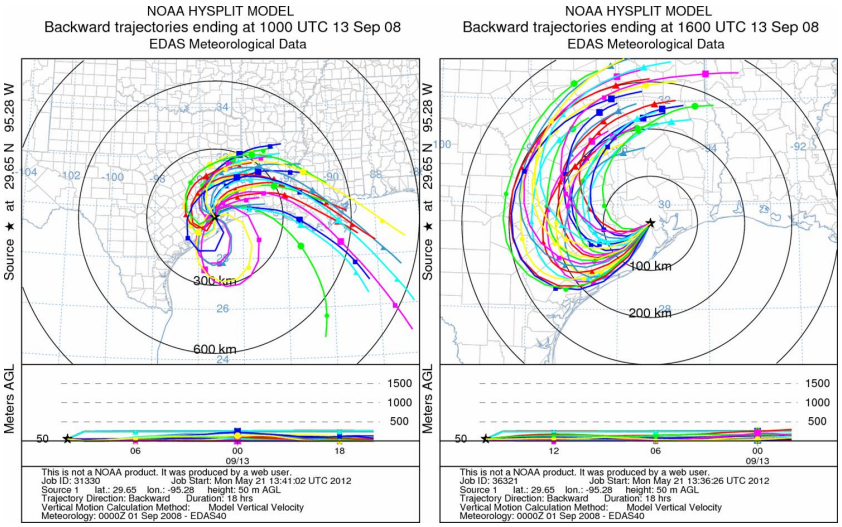

Figure 14. Back trajectory ensembles for 04:00 CST (left) and 10:00 CST (right) on DOY 257.

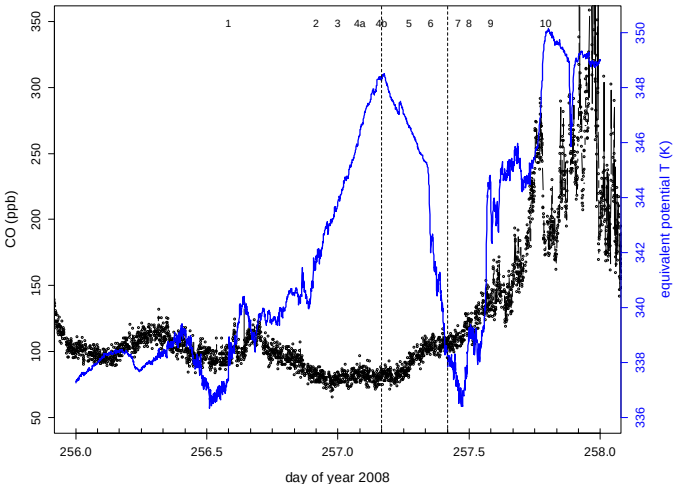

Figure 15. Time series of carbon monoxide (CO) levels as compared to Θ_e prior and during Ike's passage over Houston. As in previous Figures, rain band passage timing is indicated along the top. The two vertical dashed lines mark the start times for the back trajectories plotted in Fig. 14.

In addition to Θ_e rainfall dynamics were analyzed. A time series analyses of the storm data showed principle periodicities of 20 and 50 minutes, corresponding to rain band recurrence. For the flooding potential, the total amount and intensity of rainfall is of particular interest.

http://dx.doi.org/10.5772/51344

As Houston is flood-prone, several rain and flood gauges are maintained throughout the water sheds in the metro area. Thus, the locally measured rainfall was compared to the collection of data provided online [28] in Figure 16.

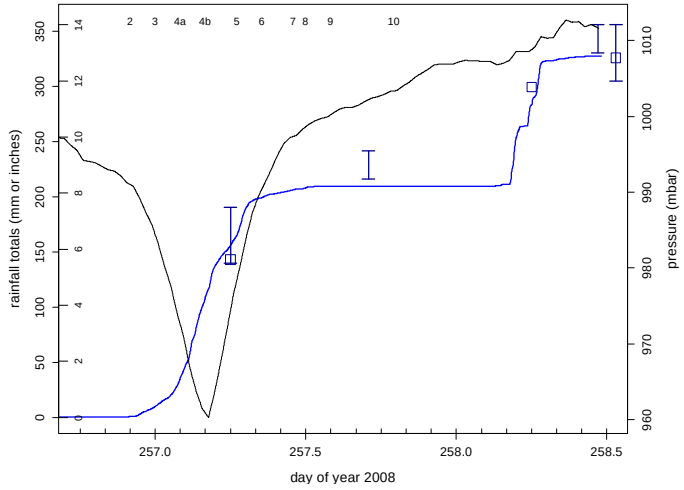

Figure 16. Rainfall development (blue line) during both Hurricane Ike's and the subsequent day's morning frontal passage over Houston. Vertical dark blue bars mark radar-derived precipitation totals, open squares mark totals observed at the nearest USGS gain gauge in the White-Oak-Bayou water shed. Pressure and rain band passage timing are plotted for orientation.

In general, a good agreement was found between the extrapolated radar data and the closest rain gauge to the tower. There appears to be a slight underestimation of the local measurements as compared to the references, which could be explained by the location of the rain gauge on the tower: As it is installed on the east side of the tower, rainfall approaching from the west and southwest during the second half of the eyewall passage may not have all reached the bucket. However, the highest rainfall rates were recorded during the NW eyewall passage consistent with the radar data [28], reaching 11 mm $(10\ min)^{-1}$. Nearly twice the intensity, 19 mm $(10\ min)^{-1}$, however, was observed during the post-storm frontal passage on DOY 258 fueled by storm-intensified humidity entrainment from the Gulf of Mexico [28], Fig. 16, which added almost as much rainfall to the total as caused by Ike during the previous day. Ultimately, a total of 327 mm (12.9 inches) of rain fell onsite within 36 hours, with up to 15 inches as estimated from the radar data for other areas of Houston [28], more than three times the long term average September rainfall for this area [46].

6. Conclusions

Hurricane Ike's path after landfall during the early morning hours on 13 September 2008 crossed through Galveston Bay, went north along the eastern border of Harris County, then

slightly northwest again towards north of Houston, until finally veering NNE towards northeast Texas. Most of Harris County, including the city of Houston and the economically important Ship Channel, went through the western, often less severe eyewall of the hurricane. Nevertheless, the Houston metro area suffered from widespread power outages caused by the hurricane's impacts hours before the highest rain rates and wind speeds passed. Onsite measured rainfall compared well with independent data. While local flooding was caused by this three-times monthly average amount in 36 hours, the Houston drainage network including its improvements since tropical storm Allison in 2001 seemingly handled the amount of water adequately [47]. The same was not the case with respect to preparations for potential wind damage. This chapter described Ike's wind field from approach to retreat as measured from a tower platform north of downtown Houston. Measured winds were likely representative of the larger metro area, showing tropical storm force winds at 20 m agl, strongly slowed by the rough urban surface as compared to standardized H*Wind products. However, although measured wind speeds were significantly lower than commonly cited, strong downward momentum fluxes in combination with high turbulence intensities, likely locally exaggerated by building wakes, caused "moderate" tree and building damage in the area equivalent to what would be expected from a category two hurricane. As this "moderate" damage dominantly occurred to a mature, poorly trimmed tree canopy in neighborhoods where power is distributed aboveground on poles, much higher than expected power line loss resulted.

Similar to previous measurements, the wind analysis results also indicate larger horizontal structures in the wind field not present at lower wind speeds. Significant interaction of these *roll* features with the underlying surface might contribute to the damage potential of the storm, but this cannot be evaluated with confidence from a single observing location. The extensive meteorological observations along the Gulf Coast during Hurricane Ike may, however, provide the opportunity for such an analysis once all data become analyzed in more detail.

Additional observations of equivalent potential temperature and air quality development during the approach and passage of Hurricane Ike revealed that Houston may have been spared even larger damage from high winds because of entrainment of drier continental air into the western eyewall. While higher wind speeds were maintained south and east of the eye, Houston in the west of the eye experienced overall lower winds and shorter durations of tropical storm force winds than observed on the east side of the eye [28].

Acknowledgements

I am indebted to the employees of Houston Yellow Cab at 1406 Hays Street, particularly William Hernandez, who were onsite during the storm to keep the power from their generator on and protect our equipment against water that had penetrated the flat roof structure shown in Fig. 12. The Greater Houston Transportation Co. has provided free access to its tower and base building for our study since 2007, thereby facilitating and supporting these unique urban measurements. We continue to be grateful for this private enterprise support of our academic goals. I also thank my graduate student Marty Hale for assembling Figure 4b. Our research

was supported at the time by the Texas Air Research Center (TARC), Lamar University, Beaumont, TX, and a start-up grant to the author by Texas A&M University in College Station.

Author details

Gunnar W. Schade

Address all correspondence to: gws@geos.tamu.edu

Department of Atmospheric Sciences, Texas A&M University, College Station, TX, USA

References

[1] Pielke, R.A., J. Gratz, C.W. Landsea, D. Collins, M.A. Saunders, and R. Musulin, Normalized hurricane damage in the United States: 1900-2005. Natural Hazards Review, 2008. 9(1): p. 29-42.

[2] Lorsolo, S., J.L. Schroeder, P. Dodge, and F. Marks, An Observational Study of Hurricane Boundary Layer Small-Scale Coherent Structures. Monthly Weather Review, 2008. 136: p. 2871.

[3] Powell, M.D., S.H. Houston, and T.A. Reinhold, Hurricane Andrew's Landfall in South Florida. Part I: Standardizing Measurements for Documentation of Surface Wind Fields. Weather and Forecasting, 1996. 11: p. 304-328.

[4] Schroeder, J.L. and D.A. Smith, Hurricane Bonnie wind flow characteristics as determined from WEMITE. Journal of Wind Engineering and Industrial Aerodynamics, 2003. 91: p. 767-789.

[5] Skwira, G.D., J.L. Schroeder, and R.E. Peterson, Surface Observations of Landfalling Hurricane Rainbands. Monthly Weather Review, 2005. 133: p. 454-465.

[6] Masters, F.J., H.W. Tieleman, and J.A. Balderrama, Surface wind measurements in three Gulf Coast hurricanes of 2005. Journal of Wind Engineering and Industrial Aerodynamics, 2010. 98(10-11): p. 533-547.

[7] Yu, B., A.G. Chowdhury, and F.J. Masters, Hurricane Wind Power Spectra, Cospectra, and Integral Length Scales. Boundary-Layer Meteorology, 2008. 129(3): p. 411-430.

[8] Doran, J.C., J.D. Fast, and J. Horel, The VTMX 2000 campaign. Bulletin of the American Meteorological Society, 2002. 83(4): p. 537-551.

[9] Chen, F., R. Bornstein, S. Grimmond, J. Li, X. Liang, A. Martilli, S. Miao, J. Voogt, and Y. Wang, Research priorities in observing and modeling urban weather and climate. Bulletin of the American Meteorological Society, 2012(in press).

[10] Changnon, S.A., INADVERTENT WEATHER-MODIFICATION IN URBAN AREAS - LESSONS FOR GLOBAL CLIMATE CHANGE. Bulletin of the American Meteorological Society, 1992. 73(5): p. 619-627.

[11] Berkowitz, C.M., S. Springston, J.C. Doran, J.D. Fast, and Ams, Vertical mixing and chemistry over an arid urban site: First results from aircraft observations made during the Phoenix sunrise campaign. Fourth Conference on Atmospheric Chemistry: Urban, Regional and Global Scale Impacts of Air Pollutants2002. 165-168.

[12] Allwine, K.J., J.H. Shinn, G.E. Streit, K.L. Clawson, and M. Brown, Overview of urban 2000 - A multiscale field study of dispersion through an urban environment. Bulletin of the American Meteorological Society, 2002. 83(4): p. 521-536.

[13] Oke, T., K. Klysik, and C. Bernhofer, Editorial: Progress in urban climate. Theoretical and Applied Climatology, 2006. 84(1-3): p. 1-2.

[14] Oke, T.R., Towards better scientific communication in urban climate. Theoretical and Applied Climatology, 2006. 84(1-3): p. 179-190.

[15] Oke, T.R., Initial guidance to obtain representative meteorological pbservations at urban sites, 2006, World Meteorological Organisation: Geneva.

[16] Roth, M., Review of atmospheric turbulence over cities. Quarterly Journal Of The Royal Meteorological Society, 2000. 126(564): p. 941-990.

[17] Schade, G.W., Relating urban turbulence and trace gas flux measurements from a tall tower to surface characteristics and anthropogenic activities, 2009, Texas A&M University: College Station. p. 42.

[18] Park, C., G.W. Schade, and I. Boedeker, Flux measurements of volatile organic compounds by the relaxed eddy accumulation method combined with a GC-FID system in urban Houston, Texas. Atmospheric Environment, 2010. 44(21-22): p. 2605-2614.

[19] CenterPoint Energy Inc. Hurricane Ike, Like many things, bigger in Texas. 2009 [cited 2012, 5 July]; Available from: http://www.centerpointenergy.com/newsroom/storm-center/ike/.

[20] Berg, R., Tropical Cyclone Report, Hurricane Ike, 1 - 14 September 2008, 2009/2010, National Hurricane Center. p. 55.

[21] Hurricane Ike Impact Report, FEMA, Editor 2008, ESF#14. p. 64.

[22] G.W., S. and B. Rappenglueck, Unique Meteorological Data During Hurricane Ike's Passage Over Houston. EOS, 2009. 90(25): p. 215-216.

[23] Fowler, T., Next hurricane may not knock out Houston power so long, Lights could be restored faster, Electric utilities apply lessons of Hurricane Ike, in Houston Chronicle 2009, Hearst Communications Inc.: Houston, Texas.

[24] Fowler, T., Lesson of Ike: Money needed for power grid vs. blackouts, Investment in grid could bring quicker power return, Task force wants new technology it says can

http://dx.doi.org/10.5772/51344

cut wait time after storm outages in Houston Chronicle 2009, Hearst Communications Inc.: Houston, Texas.

[25] Park, C., G.W. Schade, and I. Boedeker, Characteristics of the flux of isoprene and its oxidation products in an urban area. Journal Of Geophysical Research-Atmospheres, 2011. 116.

[26] Grimmond, C.S.B., T.S. King, M. Roth, and T.R. Oke, Aerodynamic roughness of urban areas derived from wind observations. Boundary-Layer Meteorology, 1998. 89(1): p. 1-24.

[27] Chambers, M., The Hurricane Severity Index – A New Method of Classifying the Destructive Potential of Tropical Cyclones, in Severe Storm Prediction and Global Climate Impact on the Gulf Coast2008, SSPEED: Rice University, Houston, TX.

[28] National Weather Service (NWS) Houston/Galveston. Hurricane Ike (2008). 2012 [cited 2012 10 June]; Available from: http://www.srh.noaa.gov/hgx/?n=projects_ike08.

[29] HGAC, 2011 Regional Storm Debris Management Assessment, 2011, Houston-Galveston Area Council (H-GAC). p. 155.

[30] Flesch, T.K. and J.D. Wilson, Wind and remnant tree sway in forest cutblocks.: I. Measured winds in experimental cutblocks. Agricultural and Forest Meteorology, 1999. 93(4): p. 229.

[31] Panferov, O. and A. Sogachev, Influence of gap size on wind damage variables in a forest. Agricultural and Forest Meteorology, 2008. 148(11): p. 1869.

[32] Powell, M.D., New findings on hurricane intensity,wind field extent, and surface drag coefficient behavior, in Tenth international workshop on wave hindcasting and forecasting and coastal hazard symposium2007: North Shore, Oahu, Hawaii. p. 14.

[33] Li, Q.S., L.H. Zhi, and F. Hu, Boundary layer wind structure from observations on a 325 m tower. Journal of Wind Engineering and Industrial Aerodynamics, 2010. 98(12): p. 818-832.

[34] Varshney, K. and K. Poddar, Experiments on integral length scale control in atmospheric boundary layer wind tunnel. Theoretical and Applied Climatology, 2011. 106(1-2): p. 127-137.

[35] R Development Core Team. R: A language and environment for statistical computing. 2012; Available from: http://www.R-project.org/.

[36] Flesch, T.K. and J.D. Wilson, Wind and remnant tree sway in forest cutblocks. II. Relating measured tree sway to wind statistics. Agricultural and Forest Meteorology, 1999. 93(4): p. 243.

[37] Wilson, J.D. and T.K. Flesch, Wind and remnant tree sway in forest cutblocks. III. a windflow model to diagnose spatial variation. Agricultural and Forest Meteorology, 1999. 93(4): p. 259.

[38] Zeng, H., H. Peltola, A. Talkkari, A. Venäläinen, H. Strandman, S. Kellomäki, and K. Wang, Influence of clear-cutting on the risk of wind damage at forest edges. Forest Ecology and Management, 2004. 203(1-3): p. 77.

[39] Dupont, S. and Y. Brunet, Simulation of turbulent flow in an urban forested park damaged by a windstorm. Boundary-Layer Meteorology, 2006. 120(1): p. 133-161.

[40] WeatherPredict Consulting Inc., Hurricane Ike Meteorological Assessment and Damage Survey, Sptember 2008, RenaissanceRe, Editor 2008.

[41] Emanuel, K., Hurricanes: Tempests in a greenhouse. Physics Today, 2006. 59(8): p. 74-75.

[42] Bell, M.M. and M.T. Montgomery, Observed structure, evolution, and potential intensity of category 5 Hurricane Isabel (2003) from 12 to 14 September. Monthly Weather Review, 2008. 136(6): p. 2023-2046.

[43] Draxler, R.R. and G.D. Rolph. HYSPLIT (HYbrid Single-Particle Lagrangian Integrated Trajectory). 2012; Available from: http://ready.arl.noaa.gov/HYSPLIT.php.

[44] Rolph, G.D. Real-time Environmental Applications and Display sYstem (READY). 2012; Available from: http://ready.arl.noaa.gov.

[45] George, C., Ike had hidden toll in gaming kids sickened by generator, in Houston Chronicle 2009, Hearst Communications Inc.: Houston.

[46] Office of the State Climatologist. 2012 [cited 2012, 5 July]; Available from: http://atmo.tamu.edu/osc/tx.

[47] Berger, E., Progress and lessons 10 years after Tropical Storm Allison, in Houston Chronicle 2011, Hearst Communications Inc. : Houston.